

Characterization of inductively coupled RF plasma source operating with molecular gases for electric propulsion

Y. A. Ussenov¹ and Y. Raitses²

Princeton Plasma Physics Laboratory, Princeton, NJ, 08540, USA

Inductively coupled radio-frequency (RF-ICP) plasma sources are widely used in semiconductor processing, mass spectrometry, nanomaterial synthesis, and also in space propulsion, where they operate across pressures from mTorr to atmospheric and power levels from tens of watts to tens of kilowatts. RF-ICPs offer an electrode-free, magnetic-field-free design that is simpler and lighter than helicon or electron-cyclotron-resonance sources, while advanced configurations with ferrite cores can achieve competitive ionization efficiency. This work develops and characterizes a low-pressure (≤ 10 mTorr), low-power (up to 250 W) RF-ICP source to maximize ionization of molecular gases with potential application to space propulsion such as plasma thrusters and cathodes with molecular propellant.

I. Nomenclature

V_p	=	plasma potential
n_e	=	electron density
T_e	=	electron temperature
V_f	=	floating potential
S_p	=	probe surface area
$f(\varepsilon)$	=	electron energy probability function
$F(\varepsilon)$	=	electron energy distribution function
$P_{app.}$	=	applied RF power
$P_{for.}$	=	forward RF power
$P_{ref.}$	=	reflected power
$P_{coup.}$	=	coupled RF power
$\langle \varepsilon \rangle$	=	mean electron energy
ε_T	=	ionization cost
Γ_i	=	ion Bohm flux
S_{loss}	=	surface loss area

II. Introduction

The Inductively Coupled radio frequency plasma sources (RF-ICP) have been extensively studied and used for industrial applications ranging from semiconductor nanofabrication at low pressures (a few mTorr to hundreds mTorr) to mass-spectroscopy at moderate pressures, and the synthesis of nanomaterials and plasma chemical decomposition of gases at sub-atmospheric (100's torr) and atmospheric pressure^{1,2}. For space propulsion, moderate (0.01-1 Torr) to atmospheric pressure ICPs were proposed and used as miniaturized low power (10's W) and scaled up (0.1-10's kW) electrothermal plasma thrusters^{3,4}. A number of studies have explored the use of low pressure (a few mTorr to 10's mTorr) 100 W-class ICP plasma sources as cathode-neutralizers for ion and Hall thrusters⁵. Additionally, there is a

¹ Associate Research Physicist, AM&SS.

² Principal Research Physicist, DPS and AM&SS, AIAA Associate Fellow.

strong need in electrodeless plasma and multimodal propulsion solutions for space applications. In this regard, RF-ICP are a reasonable choice as they are electrodeless and can, in principle, generate plasma from various relevant molecular gases including air, hydrogen, nitrogen, oxygen, NH_x , C_xH_x , Cox . Unlike their magnetically enhanced RF-ICP plasma counterparts, including helicon and electron-cyclotron resonance (ECR) plasma sources, RF-ICP operation does not require DC or additional AC magnetic fields, making its design simpler and lighter. Furthermore, advanced ICPs with improved RF coupling to plasma (e.g., ICP with ferrite core⁵) can achieve comparable or even better energy per ion-electron pair created (ion cost) as helicon and ECR plasma sources.

A majority of ICP studies for propulsion applications have involved the use of argon or argon-based gas mixtures as the propellant for RF thrusters or as working gas for RF cathodes. Advanced ICPs demonstrated efficient ionization of argon gas measured as the energy lost per electron-ion created. For example, in⁵, this so-called ionization cost for a 100 W ICP was ~ 40 eV at 0.5 mTorr of Ar. For molecular propellants such as nitrogen and oxygen, the ionization cost can increase 3-5 times compared to argon leading to inefficiency of the ICP plasma. This inefficiency is usually associated with losses due to the excitation and dissociation of molecular species and their ionization, which can be especially prominent in low-power and low-pressure operation of ICPs. For instance, the same advanced 100 W ICP described in⁵ was not able to sustain operation with nitrogen gas even at 20 times higher pressure (10 mTorr) than that required for argon operation. Thus, studying the ionization kinetics of molecular gases in RF-ICP at low pressures is crucial for further improving the application of ICP sources in electric propulsion. This includes their use in low-orbit air-breathing electric thrusters.

This work reports the development of a laboratory RF-ICP source and its preliminary characterization. The goal is to explore the limits and strategies for maximizing the ionization of molecular gases in RF-ICP plasma sources operating at low pressures and low power levels (up to hundred watts). These efforts support applications in low-power plasma propulsion technologies for space, including air-breathing plasma thrusters, RF cathodes, and RF plasma thrusters. The remainder of this paper is structured as follows: Section III describes the experimental setup and diagnostic methods employed; Section IV presents and discusses the experimental results; and Section V summarizes the main conclusions

III. Experimental setup

The general scheme of the RF-ICP plasma source shown in Figure 1. It has cylindrical shape and designed following the sources in^{6,7}. The main discharge zone of the RF-ICP plasma consists of an Al_2O_3 ceramic tube with a 90 mm inner diameter, 203 mm height, and 10 mm wall thickness. Three turns of copper tubing (0.635 mm in diameter) are wrapped around the ceramic tube, serving as the induction coils for the ICP plasma. Beneath the copper coils, several turns of plastic tubing are tightly wrapped on the ceramic surface, with deionized (DI) water supplied to both the copper and plastic tubing for effective cooling during plasma operation. The downstream vacuum chamber, with an octagonal shape and an inner diameter of 120 mm, is made of aluminum. The main discharge chamber is attached to this downstream section and can be disassembled and mounted into a larger vacuum chamber if needed. The ICP-RF plasma is ignited using an RF power supply (13.56 MHz, max 1 kW), connected to the discharge coils via an L-type matching network. Forward and reflected power are monitored directly on the RF power supply display, with a resolution of approximately ~ 1 W. Power coupling efficiency is estimated by calculating Ohmic losses in the ICP coils, determined from the ICP current measured using a Pearson current probe (model 3972) attached to the grounded side of the RF coil. Molecular gas synthetic (dry) Air (Linde Gas, 99.9999%), and reference gas Ar (Linde Gas, 99.9999%) are introduced by the gas injection ports on the top of the main discharge chamber. Their flow rates are regulated by Alicat mass-flow controllers (MC series) and the gas flow typically kept at 2 sccm. The pumping system contains turbomolecular pump (ATH 500M, Pfeiffer) and dry scroll pump (Pfeiffer, ACP 40G) connected in series to the chamber. Gas pressure within the vacuum chamber is monitored using ion (KJLC 392 Series) and convectron gauges (Granville-Philips 275 series) and controlled by adjusting a throttling gate valve at fixed incoming gas flow rate. The base vacuum pressure was $\sim 4 \times 10^{-6}$ Torr for all the experiments.

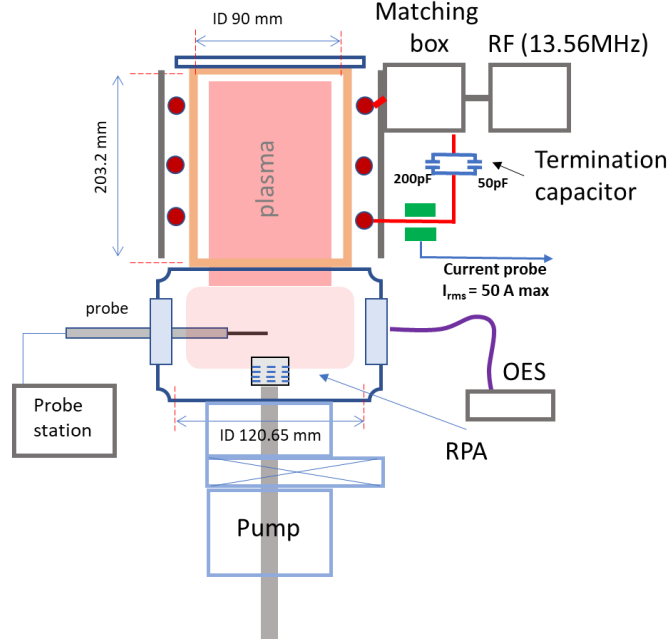


Fig. 1 The general scheme of the RF-ICP plasma source.

Plasma parameters are measured with an automated cylindrical RF-compensated Langmuir probe (PlasmaSensors) with a tungsten tip of 0.228 mm diameter and 7 mm length. The probe has RF pick-up electrode and two pairs of self-resonant chokes designed to filter out the RF signal at fundamental 13.56 MHz and higher harmonics. The probe is inserted radially from one of side vacuum ports of the downstream chamber, with the tip positioned at the central axis of the chamber. The electron energy probability function (EEDF) obtained from the second derivative of the probe characteristics following expression⁸:

$$f(\varepsilon) = \frac{2\sqrt{2m}}{S_p e^3} \times \frac{d^2 I_p}{dV^2}, \quad (1)$$

where $\frac{d^2 I_p}{dV^2}$ second derivative of the probe IV curve, which is related to the electron energy distribution function (EEDF) through the relation $F(\varepsilon) = \varepsilon^{1/2} f(\varepsilon)$. Effective electron temperature and electron density are:

$$T_e = \frac{2}{3} \langle \varepsilon \rangle = \frac{2}{3n} \int_0^\infty \varepsilon^{3/2} f(\varepsilon) d\varepsilon, \quad (2)$$

$$n_e = \int_0^\infty \varepsilon^{1/2} f(\varepsilon) d\varepsilon. \quad (3)$$

V_p is defined with respect to the grounded chamber wall and determined from the zero crossing of the second derivative of the Langmuir probe current. Note that all plasma parameters from the Langmuir probe were measured at the center of the downstream discharge zone.

The ion energy distribution function (IEDF) was measured with a retarding potential analyzer (RPA) inserted from the bottom of the downstream chamber, with the collecting orifice plane located at the bottom edge (exit) of the downstream chamber (Figure 1). The RPA consists of four grids: the first grid was grounded, the second was biased to - 50 V to repel plasma electrons, the third was scanned from 0 to 150 V to discriminate ions by energy, and the fourth was biased to - 8 V to suppress secondary electron emission. The ion current was collected on a grounded collector and measured with an oscilloscope, and the first derivative of the current signal was normalized to compare IEDFs across different experimental conditions.

The general photo of the RF-ICP plasma source in operation is shown in Figure 1 in synthetic (dry) Air and Ar at $P_{app.} = 150$ W and 1 mTorr.

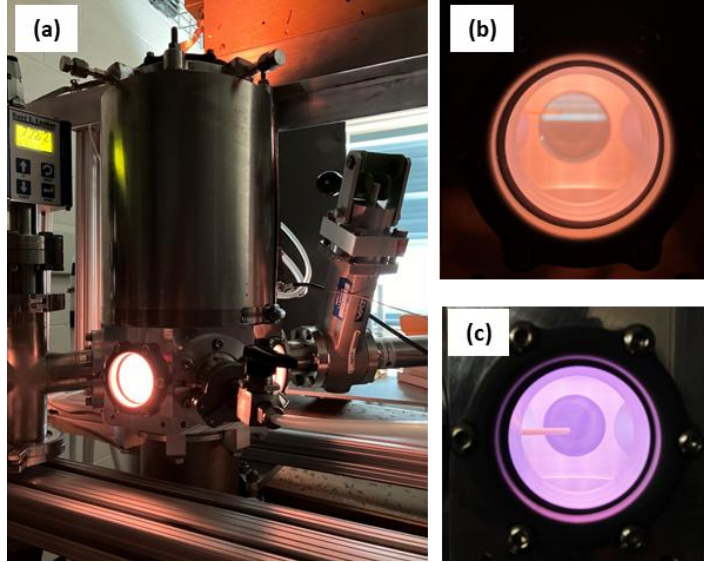


Fig. 2 RF-ICP plasma source (a) in operation with dry Air (b) and Ar (c) at 150W and 1 mTorr.

IV. Results and discussion

The RF-ICP plasma sources usually operate in so called E and H modes⁹ depending on the power coupling mechanism from RF antenna to the plasma¹⁰. The low-power E-mode is dominated by capacitive coupling, where power is mainly deposited through the electrostatic field between the antenna coil and the grounded chamber, and electrons are heated by oscillating sheaths at the plasma boundaries, resulting in relatively low plasma density in main discharge zone and strong bombardment of the walls that causes significant sputtering. In contrast, the high-power H-mode relies on inductive coupling, with power transferred to plasma via the electromagnetic field induced by the RF current in the coil, so that azimuthal electric fields drive collisional (Joule) heating of electrons throughout the bulk, producing substantially higher electron and plasma densities while reducing sheath-related wall sputtering. The transition from E- to H-mode¹¹ typically exhibits hysteresis, reflecting the nonlinear dependence of power absorption and plasma conductivity on electron density, so that the power level required to ignite H-mode is higher than the power at which it can be sustained when ramping down. A standard way to cut down unwanted E-mode coupling is to place a grounded Faraday shield between the coil and the plasma, but this makes low-power ignition harder and requires very careful mechanical design. Another option is to add a termination capacitor between the coil and ground, which reshapes the voltage along the coil and lowers its effective potential relative to the chamber^{12,13}. Choosing the capacitor so its reactance is on the order of half the coil's inductive reactance gives a low-impedance return for RF current, flattening the coil voltage profile and suppressing the capacitive field that drives E-mode. This reduces RF fluctuations of the plasma potential and makes Langmuir probe measurements much cleaner and less distorted. Thus, to reduce capacitive coupling of the RF field to the plasma, an additional termination capacitor $C_{\text{ter}} = 250$ pF is connected in series between the lower end of the coil and ground. The plasma parameters are then evaluated in two regimes: with reduced capacitive coupling when C_{ter} is included in the coil circuit, and with stronger capacitive coupling when the termination capacitor is absent. Note that adding the termination capacitor increases the likelihood of transitioning to H-mode coupling, but does not guarantee it, because the actual transition still depends on the working gas, plasma conditions, and applied RF power level. To evaluate the reduction of plasma RF fluctuations, the floating potential of a large cylindrical probe (6.35 mm in diameter and 70 mm in length) was measured with an oscilloscope. As an example, the peak amplitudes of the RF component at a given set of synthetic-air plasma parameters are summarized in Table 1. The data show that the RF

plasma fluctuations decrease by roughly a factor of ~ 20 , from $V_{\text{peak}} = 30.0$ V down to 1.6 V. This strong reduction indicates that adding the termination capacitor promotes a transition from E-mode to H-mode coupling.

Table 1. Peak value V_{peak} of the RF component of floating potential of the large probe at some discharge parameters

Power, W	Pressure, mTorr	V_{peak} (w/o C_{ter} cap.)	V_{peak} (with 250 pF cap.)
50	100	19.2	1.0
100	10	29.0	1.6
100	100	30.0	1.6

One of the main characteristics of RF-ICP sources is power coupling efficiency. At interested operation parameters RF power coupling in ICP sources is inherently below 100%, because a fraction of the applied RF power is unavoidably lost in the coil, dielectric window, matching network, and other circuit elements rather than being absorbed by the plasma. The coupling efficiency is determined by the complex plasma impedance (e.g. by density, gas composition and pressure) and by the antenna and chamber geometry, which together control how well the RF power are matched to the time-varying plasma load. The efficiency was defined as:

$$\text{Coupling efficiency} = \frac{P_{\text{coup}}}{P_{\text{app}}} \times 100\%, \quad (4)$$

where $P_{\text{app}} = P_{\text{forw}} - P_{\text{ref}}$, and $P_{\text{coup}} = P_{\text{app}} - I_{\text{coil}}^2 \times R_{\text{coil}}$. The root mean square (rms) value of the coil current I_{coil} measured during the discharge operation with Pearson current probe. The total resistance of the coil and network R_{coil} estimated by applying the RF power to the coil without the plasma ignited (at base vacuum pressure $\sim 10^{-6}$ Torr), by measuring the coil current I_{coil} respect to the different P_{app} . From the slope of the linear fit of the plot I_{coil}^2 versus P_{app} the estimated value of $R_{\text{coil}} = 0.17 \pm 0.02 \Omega$ obtained, which is further used for calculation of the Ohmic losses during the discharge operation.

The power coupling efficiency was determined for Ar and air over an applied RF power range P_{app} up to 250 W at gas pressures of 0.3, 1, and 10 mTorr. For Ar, the results with and without the termination capacitor are presented in Figure 3(a) and 3(b), respectively. Increasing the pressure improves the coupling efficiency, reaching about 80% at 10 mTorr and 30 - 50% at 1 mTorr, whereas at 0.3 mTorr the efficiency remains low. A gradual rise in efficiency is also observed as P_{app} increases from 100 to 250 W.

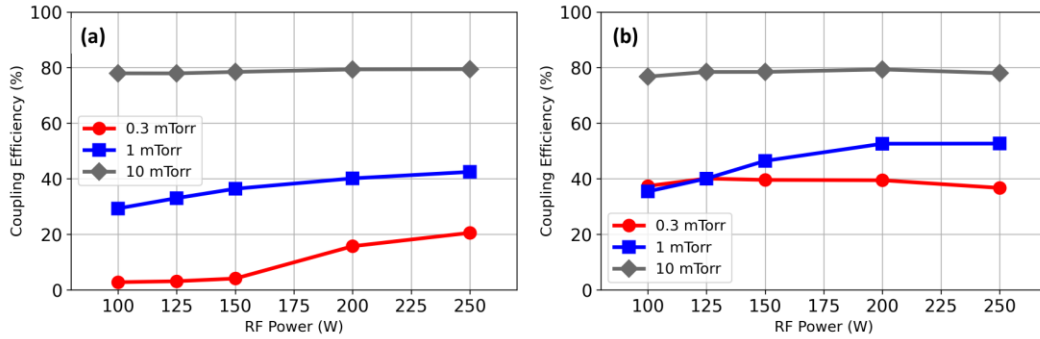


Fig. 3 Power coupling efficiency of the RF-ICP in Argon with (a) and without (b) termination capacitor.

Similar trends were obtained for dry air, as shown in Figure 4. However, at comparable pressures and applied powers, the coupling efficiency in air is consistently lower than in argon.

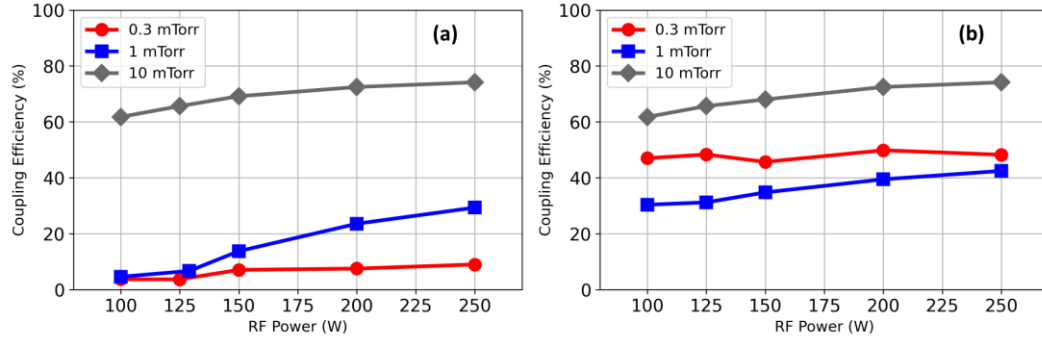
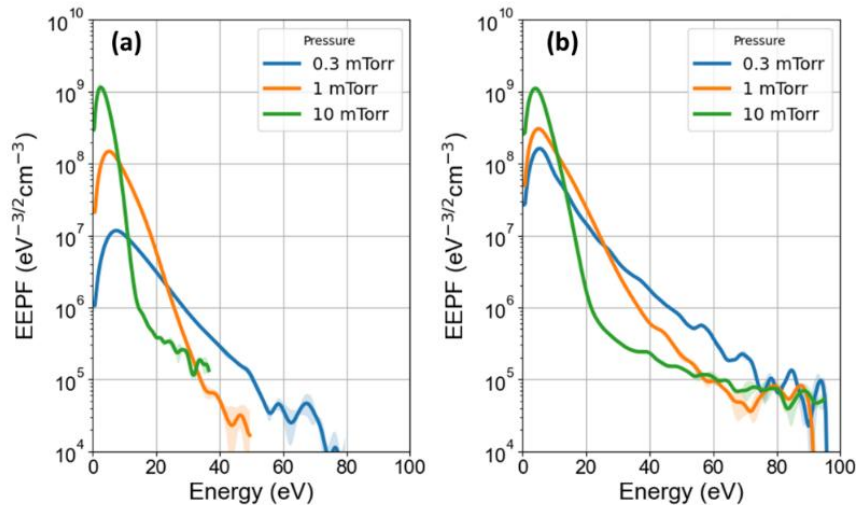


Fig. 4 Power coupling efficiency of the RF-ICP in dry Air with (a) and without (b) termination capacitor.

RF power coupling in ICPs is low at reduced gas pressure because both the electron - neutral collision frequency and the electron density are small, giving low plasma conductivity and weak induced RF currents, so most of the applied RF power is lost in the coil and hardware rather than as Ohmic heating in the plasma¹⁴. As the pressure increases, more frequent collisions and stepwise ionization raise the electron density and effective conductivity, the plasma load becomes better matched to the antenna, and a larger fraction of the RF power is absorbed in the plasma, so the coupling efficiency increases^{15,16}. The lower coupling efficiency in dry air than in argon at similar discharge conditions is primarily due to the reduced plasma density in air: ionizing air is harder because its molecular components introduce additional inelastic energy - loss and electron-loss channels, so more RF power goes into non-ionizing processes. Furthermore, the electronegativity of O₂ causes negative-ion formation via electron attachment and molecular ions are efficiently removed by dissociative recombination, both of which deplete the free-electron population and further limit the achievable plasma density.

The EEPFs of Ar and dry air plasmas in the RF ICP, with and without the termination capacitor, were measured over 0–100 eV electron energy range and used to extract the corresponding plasma parameters at different pressures (Figure 5 and Table 2). The measurements cover a wide electron density range of $\sim 10^5 - 10^9 \text{ cm}^{-3}$ with negligible noise. As expected, increasing the gas pressure reduces the electron temperature T_e from $\sim 10 \text{ eV}$ down to $\sim 2.5 \text{ eV}$ for Ar and from $\sim 16 \text{ eV}$ down to $\sim 4.3 \text{ eV}$ in for dry Air for both discharge configurations. Meanwhile, the electron density rises from $\sim 5.5 \times 10^8 \text{ cm}^{-3}$ up to $\sim 1.6 \times 10^{10} \text{ cm}^{-3}$. The reduction in electron temperature and rise of the electron density with increase of the gas pressure is consistent with global discharge model. As the gas pressure increases, electron - neutral collision frequency rises, so electrons lose energy more efficiently to excitation, ionization, and gas heating, which cools the electron population and lowers the electron temperature. At the same time, at fixed input power and certain pressure ranges, these frequent collision events and the reduced diffusion losses at higher pressure produce more ionization and better particle confinement, so the electron density increases even though electron population is colder.



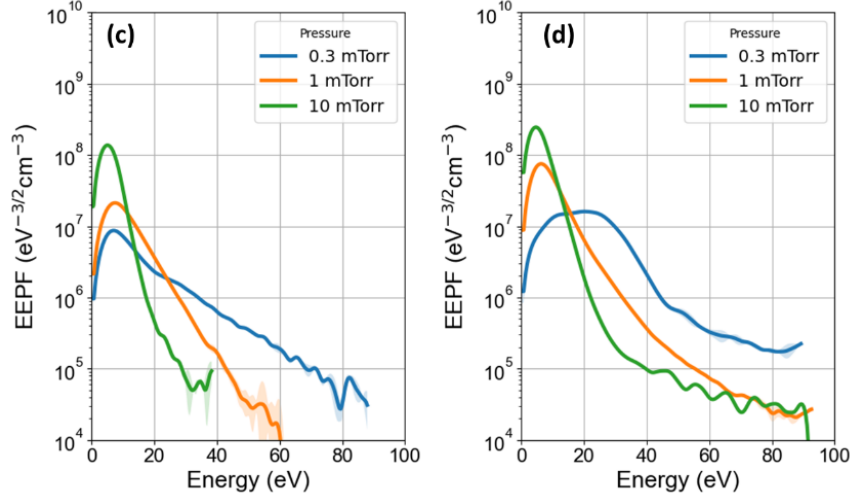


Fig. 5 EEPF in RF-ICP at 150W applied power in Ar (top) and dry Air (bottom) with (a,c) and without (b,d) termination capacitor.

The EEPF comparison between the purely capacitive and reduced-capacitive configurations shows that, in the reduced-capacitive mode, the high-energy tail is more strongly populated. This behavior is consistent with enhanced stochastic heating of electrons in the capacitive sheaths at 0.3 and 1 mTorr, which efficiently generates energetic electrons. In most conditions the EEPFs are close to Maxwellian, but at 10 mTorr a clear two-temperature (bi-Maxwellian-like) structure appears for both Ar and air, in both coupling configurations, indicating the coexistence of cold and hot electron populations. While bi-Maxwellian EEDFs are often attributed to collisionless stochastic heating at low pressure¹⁷, here the 10 mTorr behavior is more plausibly linked to nonlocal electron kinetics and spatial separation between the main discharge and downstream regions and thus warrants more detailed future investigation.

Table 2. Plasma parameters at 150W

Argon	C termination			no termination		
	T_e , eV	n_e , cm ⁻³	V_p , V	T_e , eV	n_e , cm ⁻³	V_p , V
Pressure, mTorr						
0.3	10.0±0.4	5.5e+08	71.5±3.01	8.2±0.4	4.5e+09	86.9±0.3
1	5.4±0.3	3.43e+09	19.2±0.9	6.5±0.3	8.0e+09	77.1± 0.4
10	2.5±0.3	9.50e+09	7.8± 0.3	3.8±0.4	1.6e+10	31.9± 1.3
Air	C termination			no termination		
	T_e , eV	n_e , cm ⁻³	V_p , V	T_e , eV	n_e , cm ⁻³	V_p , V
Pressure, mTorr						
0.3	14.4±0.2	5.2e+8	91.2±0.7	16.5±0.3	1.93e+09	116.4± 0.7
1	8.4±0.1	8.06e+08	48.6±2.4	7.1±0.5	2.15e+09	67.9±0.1
10	4.3 ±0.1	2.13e+09	20.7±1.1	4.3±0.5	4.03e+09	58.2±0.3

With the known coupled plasma power P_{coup} and n_e and T_e , we can estimate the ionization cost $\varepsilon_T \approx P_{\text{coup}}/\Gamma_i S_{\text{loss}}$ per ion-electron pairs, where $\Gamma_i = 0.6 n_e (k_B T_e / m_i)^{1/2}$ ion Bohm flux at the sheath edge near the wall surface. Let us consider the 10 mTorr case, where high plasma density and the absorbed power efficiency observed. Assuming total

$S_{loss} \approx 0.1 \text{ m}^2$, and $P_{coup} \approx 120 \text{ W}$, $n_e = 1.6 \times 10^{10} \text{ cm}^{-3}$, $T_e = 3.8 \text{ eV}$, the ion energy cost for Ar is $\sim 4 \times 10^{-17} \text{ J/ion}$ or $\sim 250 \text{ eV/ion}$. Doing the same estimations for dry air (assuming the N_2 as main gas) for $n_e = 4.0 \times 10^{19} \text{ cm}^{-3}$, $T_e = 4.3 \text{ eV}$ we obtain $\epsilon_T \sim 1.2 \times 10^{-16} \text{ J/ion}$ or $\sim 780 \text{ eV/ion}$, which is roughly three times higher than for Ar. These ϵ_T values might be overestimated taking the fact that the plasma parameters measured at the downstream discharge zone, where the plasma density might be several times less than in the main upstream ICP discharge region. However, these results confirm that the ion energy cost is several times higher for the molecular gases (e.g. dry air) and ICP properties need to be further studied and optimized to enhance the energy efficiency of the discharge.

The results of the Langmuir probe measurements show that the addition of the termination capacitor into the coil circuit has significant impact on the plasma potential. In general, plasma potential values follow the electron temperature trends and falls with increasing gas pressure. However, the result shows that in pure capacitive mode it can be significantly enhanced (Table 2). For instance, at 1 mTorr in Ar the V_p is $\sim 19 \text{ V}$ in the reduced capacitive coupling mode (when C_{ter} inserted into the coil circuit), while in pure capacitive mode it rises to $\sim 77 \text{ V}$. The similar trend observed for dry Air and confirmed the rise of the V_p from $\sim 48 \text{ V}$ up to the $\sim 68 \text{ V}$ in the capacitive coupling regime. In capacitive mode, the antenna - plasma coupling is dominated by the RF sheath, so most of the applied RF voltage drops across sheaths at the window and walls, driving the time-averaged plasma potential to high values and causing large RF swings that probes see as a strongly oscillating floating potential. When the discharge transitions to reduced capacitive coupling or H mode, bulk Joule heating in a plasma shields the antenna voltage, the edge sheaths thin, and both the DC plasma potential and its RF oscillation amplitude drop toward a few T_e above ground. Reducing capacitive coupling with termination capacitor therefore directly lowers the RF plasma potential and stabilizes the floating potential, which then follows the smaller $V_p(t)$ excursions characteristic of H-mode operation.

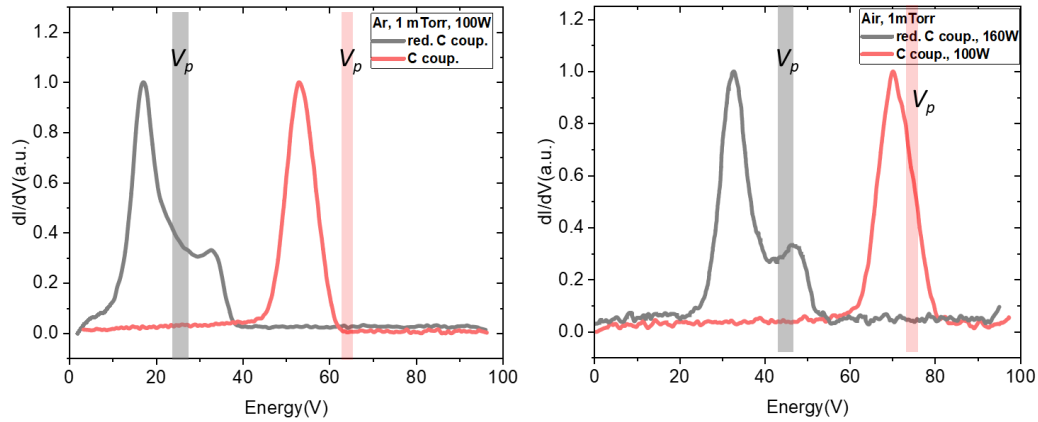


Fig. 6 IEDF measured by RPA at the exit of the downstream chamber in Ar and Air for different power coupling conditions. The vertical lines show the corresponding plasma potential V_p values in horizontal axis.

A large plasma potential relative to the chamber wall can be exploited to extract more energetic ions from the bulk plasma, which is beneficial for electric propulsion applications^{18,19}. For this reason, the IEDF was measured at the exit of the downstream chamber; the results for Ar and air at 1 mTorr are shown in Figure 6. In the capacitive coupling mode, the maximum ion energies reach about $\sim 52 \text{ eV}$ in Ar and $\sim 70 \text{ eV}$ in air, with the peak energies lying slightly below the plasma potential measured at the discharge center because of the different measurement locations and collisional energy losses during ion transport, yet still closely following the overall plasma-potential trend. In the reduced capacitive coupling mode, the IEDF exhibits two distinct peaks: a dominant low-energy peak below the local plasma potential and a secondary peak higher by roughly $\sim 17\text{--}18 \text{ eV}$, attributed to ions originating from the main ICP (upstream) region and arriving at the downstream exit after partial collisional slowing. In capacitive mode, the plasma - and hence the plasma potential - is distributed relatively uniformly between the main discharge and downstream zones along the RF electric-field lines, whereas in the reduced-capacitive (H-mode-like) configuration the plasma is primarily localized near the coil where the azimuthal electric field is strongest, leading to two spatially separated discharge regions whose ion populations are both sampled at the downstream exit. The lower intensity of the high-energy IEDF peak is consistent with collisional attenuation of upstream ions in transit, and similar double-peaked IEDFs have been reported previously in simple ICP²⁰ sources and in helicon discharges²¹. Considering the peak ion energies $E_{i,Ar} = 52 \text{ eV}$ and $E_{i,Air} = 70 \text{ eV}$, the corresponding ion velocities are

$V_{i,Ar} \approx 1.6 \times 10^4$ m/s and $V_{i,Air} \approx 2.2 \times 10^4$ m/s. The ionization fraction $\alpha \approx n_i/n_n$ for Argon and dry air at 1 mTorr are $\sim 2.5 \times 10^{-4}$ and $\sim 6.7 \times 10^{-5}$, respectively. Assuming, for simplicity, that the neutral gas atoms have very low velocity, that the atomic and ionic masses are similar, and that the exhaust cross-sectional area A is the same, the specific impulse can be written as $I_{sp} \approx V_{eff}/g_0$, where $V_{eff} \approx (\dot{m}_i/\dot{m}_n)V_i$ is the effective exhaust velocity, $\dot{m}_i \sim n_i m_i A V_i$ is ion mass flow rate and \dot{m}_n is total input mass flow rate. Under these assumptions, the resulting specific impulse I_{sp} is expected to remain very low, primarily because only a small fraction of the supplied gas is converted into fast, directed ions under the present operating conditions. Consequently, improvements in ionization efficiency would be required before such an RF-ICP source could serve as a competitive primary thruster in electric propulsion systems. However, even with a low specific impulse, an ICP discharge may still be acceptable - and even advantageous - as an RF cathode or plasma source, particularly when operating with air or other molecular gases where robust, electrode-less plasma generation and reliable electron supply are more critical.

V. Conclusion

This work developed and characterized a low-pressure, low-power RF-ICP source aimed at efficient ionization of molecular gases for electric-propulsion applications such as RF cathodes and air-breathing thrusters. Using Langmuir probes, a retarding potential analyzer, and power/current measurements, the study quantified power-coupling efficiency, plasma parameters, and ion energy distributions in Ar and dry air over 0.3–10 mTorr and up to 250 W. Introducing a 250 pF termination capacitor strongly reduced capacitive coupling, lowered RF plasma-potential oscillations by about an order of magnitude, and modified the plasma potential in ways consistent with a transition toward inductive (H-mode-like) operation. The coupling efficiency increased with pressure and power, reaching $\sim 80\%$ in Ar at 10 mTorr but remaining systematically lower in air due to higher ionization cost and additional loss channels in molecular gases. EEPF and IEDF measurements showed pressure-driven electron cooling with rising density, occasional bi-Maxwellian-like electron populations, and the coexistence of low- and high-energy ion groups, indicating nonlocal electron kinetics and favorable conditions for energetic-ion extraction from the upstream discharge. In particular, the high ion energies observed in the capacitive coupling regime, if combined with improved ionization efficiency, could be leveraged to develop gridless, neutralizer-less RF-ICP propulsion concepts that directly exploit high plasma potential for efficient ion acceleration. Even with a low specific impulse, an ICP discharge can still be suitable as an RF cathode or plasma source, particularly in air or other molecular gases where robust electrode-less operation and reliable electron supply are more important than high thrust efficiency.

Acknowledgments

This work was in part supported by the AFOSR Space Propulsion and Power portfolio, FA9550-25-1-0071. The authors acknowledge Prof. V. Donnelly for helping with the plasma source design. They also thank Mr. T. Bennet and Mr. A. Merzhhevskiy for technical support.

References

- ¹ Yin Y., Messier J., Hopwood J.A., “Miniaturization of inductively coupled plasma sources”, *IEEE Transactions on Plasma Science*, Vol. 27, 1999, p. 1516
- ² Alrebh, A., D. Ruth, M. Plunkett, L. Gaburici, M. Couillard, T. Lacelle, C. T. Kingston, and K. S. Kim. "Boron nitride nanotubes synthesis from ammonia borane by an inductively coupled plasma." *Chemical Engineering Journal*, Vol. 472, 202, p. 144891 <https://doi.org/10.1016/j.cej.2023.144891>
- ³ Tsifakis, D., Charles, C., and Boswell, R. (2020). “An inductively coupled plasma electrothermal radiofrequency thruster” *Frontiers in Physics*, Vol. 8, 2020, p. 34. <https://doi.org/10.3389/fphy.2020.00034>
- ⁴ Brewer L., Frind G., and Karras T., “Preliminary results of a high-power RF thruster test”, in 25th AIAA Joint Propulsion Conference, AIAA-1989-2382, Monterey, CA, USA, 12–16 July (AIAA, 1989)
- ⁵ Godyak V., Raitsev Y. and Fisch N. J., “RF Plasma Cathode-Neutralizer for Space Applications”, IEPC-2007-266, 30th International Electric Propulsion Conference, September 17-20, 2007, Florence, Italy.
- ⁶ Shin, H., Zhu, W., Donnelly, V. M., and Economou, D. J., “Surprising importance of photo-assisted etching of silicon in chlorine-containing plasmas”, *Journal of Vacuum Science & Technology A*, Vol. 30, (2012), p. 021306. <https://doi.org/10.1116/1.3681285>
- ⁷ Shin, H., Zhu, W., Xu, L., Donnelly, V. M., and Economou, D. J., “Control of ion energy distributions using a pulsed plasma with synchronous bias on a boundary electrode” *Plasma Sources Science and Technology*, Vol. 20., No. 5, 2011, p. 055001. <http://dx.doi.org/10.1088/0963-0252/20/5/055001>

-
- ⁸ Godyak, V. A., Piejak, R. B. and Alexandrovich, B. M., “Electron energy distribution function measurements and plasma parameters in inductively coupled argon plasma” *Plasma Sources Sci. Technol.*, Vol. 11, 2002, pp. 525-543, DOI 10.1088/0963-0252/11/4/320
- ⁹ Lee H.-C., Kim D.-H., Chung C.-W., “Discharge mode transition and hysteresis in inductively coupled plasma”. *Appl. Phys. Lett.* Vol. 102, No. 23, 2013, p. 234104. <https://doi.org/10.1063/1.4809925>
- ¹⁰ Turner M. M. and Lieberman M. A., “Hysteresis and the E-to-H transition in radiofrequency inductive discharges”, *Plasma Sources Sci. Technol.* Vol. 8, 1999, p. 313, DOI 10.1088/0963-0252/8/2/312
- ¹¹ Mitsui Y., and Makabe T., “Review and current status: E \rightleftharpoons H mode transition in low-temperature ICP and related electron dynamics” *Plasma Sources Sci. Technol.* Vol. 30, 2021, p. 02300. DOI 10.1088/1361-6595/abd380
- ¹² Edamura M., Benck E. C., “Effects of voltage distribution along an induction coil and discharge frequency in inductively coupled plasmas”, *J. Vac. Sci. Technol. A* Vol. 22, No. 2, 2004, p. 293–301. <https://doi.org/10.1116/1.1641052>
- ¹³ Godyak V. A., Alexandrovich B. M., “Power measurements and coupler optimization in inductive discharges” *Rev. Sci. Instrum.* Vol. 88, No. 8, 2017, p. 083512. <https://doi.org/10.1063/1.4995810>
- ¹⁴ Hopwood J., “Planar RF induction plasma coupling efficiency”, *Plasma Sources Sci. Technol.* Vol. 3, 1994, p.460 DOI 10.1088/0963-0252/3/4/002
- ¹⁵ Zielke, D., Briefi, S., and Fantz, U. “RF power transfer efficiency and plasma parameters of low-pressure high power ICPs” *Journal of Physics D: Applied Physics*, Vol. 54, No. 15, 2021, p. 155202. DOI 10.1088/1361-6463/abd8ee
- ¹⁶ Zhang X., Zhang Z., Cao J., Liu Y., Yu P.C., “The influence of gas pressure on E \leftrightarrow H mode transition in argon inductively coupled plasmas”, *AIP Advances*, Vol. 8, No. 3, 2018, p. 035121. <https://doi.org/10.1063/1.5012560>
- ¹⁷ Godyak, V. A., Piejak, R. B., and Alexandrovich, B. M. “Electron energy distribution function measurements and plasma parameters in inductively coupled argon plasma”, *Plasma Sources Sci. Technol.* Vol. 11, 2002, p. 525. DOI 10.1088/0963-0252/11/4/320
- ¹⁸ Zadiriev, I. I., Vavilin, K. V., Kral’kina, E. A., Nikonov, A. M., and Shvydkii, G. V. “Physical Properties of a Low-Power Helicon Source Operating on a High-Frequency Discharge with a Capacitive Component” *Plasma Physics Reports*, Vol. 49, No. 7, 2023, p. 890-900. <https://doi.org/10.1134/S1063780X23600536>
- ¹⁹ Dunaevsky A., Raitses Y., Fisch N. J., “Plasma acceleration from radio-frequency discharge in dielectric capillary”, *Appl. Phys. Lett.* Vol. 88, No., 25, 2006, p. 251502. <https://doi.org/10.1063/1.2214127>
- ²⁰ Park W., Tolmachev Yu. N., Volynets V. N., Pashkovskiy V. G., “Production of energetic ions in plasma by ambipolar fields: Application to etching” *J. Vac. Sci. Technol. A*, Vol. 25, No. 4, 2007, 726–730. <https://doi.org/10.1116/1.2743647>
- ²¹ Plihon N., Chabert P., Corr C. S., “Experimental investigation of double layers in expanding plasmas” *Phys. Plasmas*, Vol. 4, No. 1, 2007, p. 013506. <https://doi.org/10.1063/1.2424429>